Design of motor/generator for Flywheel Batteries

This article has been accepted for publication in a future issue of this journal, but has not been fully edited. Content may change prior to final publication. Citation information: DOI 10.1109/TIE.2020.3026292, IEEE Transactions on Industrial Electronics

Design of motor/generator for Flywheel Batteries

Claudio Bianchini, *Member, IEEE*, Ambra Torreggiani, Danilo David, and Alberto Bellini, *Senior Member, IEEE*

***Abstract*—Energy storage is an emerging technology that can enable the transition towards renewable-energy-based distributed generation, reducing peak power demand and the time difference between production and use. The energy storage could be implemented both at grid level (concentrated) or at user level (distributed). Chemical batteries represent the *de facto standard* of storage systems for performance and maturity; however, batteries feature a quite large environmental footprint and use precious raw materials. Mechanical storage technologies could represent a viable alternative to chemical batteries, because of their reduced impacts on the environment and on raw materials.**

This paper presents the design of a motor/generator for a flywheel energy storage at household level. Three reference machines were compared by means of Finite Element Analysis (FEA): a traditional iron-core surface permanent-magnet (SPM) synchronous machine, a synchronous reluctance machine (SynchRel) and an ironless SPM synchronous machine.

Simulation show that the ironless machine is good candidate for distributed energy storage, because of its high efficiency, high discharge duration and low losses. A prototype ironless machine was designed and manufactured. Experiments confirm the simulation results.

***Index Terms*—Ironless permanent magnet machines, energy storage, Climate assessment**

I. Introduction

Energy storage is a key technology to enable the transition to renewable-energy-based distributed generation systems. It can reduce peak power demand and it helps to overcome the time difference between energy production and use.

Nowadays, the emerging consensus is that the energy storage could be considered the pivotal technology that will reshape the energy sector by enabling the widespread adoption of solar and wind system connected to the grid. Storage energy could change the traditional concept of energy industry, reducing the peaks in demand of electric power in the daytime and the requirement of additional power plants. With suitable energy storage, commercial and residential consumers can become power generators and then select the price point at which they will consume electricity. With suitable energy storage, utilities and grid management can couple producers and consumers with disparate temporal behaviours, thus reducing electric power peaks and the need for additional power generation plants. The renewable energy time-shift stands for a specific value proposition where storage is charged with low-value electric energy generated using renewable energy. That energy is stored so that it may be used or sold at a later time when it is more valuable [1], [2]. The storage also results in environmental advantages as it prevents losses from transmission and dispatching and it reduces peak power demand.

Renewable energy is a breakthrough in power distribution systems, as it is a small-medium sized, distributed and intermittent energy source, i.e. it is entirely different in nature from actual energy sources, which are concentrated in a few large plants. A distributed energy storage system is best suited to distributed energy sources for two main reasons: (1) it avoids the use of huge energy storage systems, as the storage size is critical for any technology, (2) the transmission and dispatching losses are prevented. Transmission and dispatching losses range between $5\ \%$ of the total electricity generated in OECD countries and up to $20\ \%$ in developing countries.

Energy storage could be implemented at grid level, or at user level. In this paper, the feasibility and performance of different technologies for mechanical energy storage at household level were investigated.

Different technologies can be used for energy storage. Chemical batteries are the standard-de-facto in terms of performance and technology maturity, however they feature a quite large ecological footprint and a quite low lifetime; they require precious raw materials. In this paper, a flywheel (mechanical) battery is investigated, with special reference to the electric motor/generator concept.

In a domestic/residential use scenario, flywheel storage capacity and self-discharge duration are critical parameters, assuming that flywheel storage is used in combination with a photovoltaic system for a typical residential user [3]. A few hours of self-discharge duration are required to match requirements for renewable energy time-shift. The self-discharge duration is the time span in which the storage provides its rated output without recharging. Flywheel storage capacity depends on the moment of inertia and squared angular speed. In order to reach a typical household energy capacity, an high rotational speed and high discharge duration are required.

For a flywheel, self-discharge time is mainly affected by mechanical losses, core losses and windage losses, hence the design of the electrical machine used as motor/generator

Manuscript received Month xx, 2xxx; revised Month xx, xxxx; accepted Month x, xxxx. This work was supported in part by EIT Climate-KIC.

C. Bianchini and A. Torreggiani are with DIEF, University of Modena and Reggio Emilia, Reggio Emilia, ITALY, (claudio.bianchini@unimore.it, ambra.torreggiani@unimore.it).

D. David is with Raw Power s.r.l, Reggio Emilia, ITALY (danilo.david@rawpowergroup.it).

A. Bellini is with DEI, University of Bologna, Cesena, ITALY (a.bellini@unibo.it).

is critical. An iron-core brushless surface permanent-magnet could be a nice option for its high efficiency, however at high speeds it is prone to high core losses. Moreover, in iron-core machines eddy currents results in self-braking during idle operations, i.e. when the flywheel is spinning without power supply.

The shortcomings linked to core losses can be overcome with an ironless machine topology or with a pure reluctance machine. The ironless permanent-magnet machine configuration features higher reluctance of the magnetic paths, hence lower power density and efficiency than iron-core configuration. In order to overcome the reluctance drawbacks, this paper investigates a dual rotor configuration for an ironless radial surface permanent-magnet machine. This machine was designed and optimized for a flywheel energy storage at household level and then a prototype, named MechSTOR [4], was realized and tested. The MechSTOR prototype was compared with two reference machines with identical size and torque, showing that the ironless machine is best suited to the flywheel, because of increased performances in terms of discharge duration and of annual energy storage.

The paper is organized as follows, section II briefly reviews the global challenge of climate change and the role of energy storage as enabling technology towards zero-emission energy. Section III states the specification for a motor/generator used for flywheel battery in a household. Section IV reports the design of the three machines, the optimization for the MechSTOR prototype, and the performance analysis based on FEA. Section V reports a benchmark analysis of the three machines based on annual energy storage potential. The latter is used to find the optimal machine choice in a multi-variable system. Section VI reports experimental results for the MechSTOR prototype and section VII draws some conclusions.

II. Energy storage and the climate challenge

Energy is a key field for both economic and environmental point of views. It is the enabling infrastructure of our society: wealthier countries and efficient companies must be close to a cheap and continuously available energy source. Energy is also the main source of greenhouse gas emissions [5], thus the transition towards renewables (decarbonization) shall be a major target for academia, public policies and industry. Transitioning from traditional fossil-energy-based centralized power systems to renewable-energy-based distributed generation has been hampered by the cost of renewable energies - that is reducing - and by their intermittent and intrinsic unpredictability, which reduces availability and induces grid instability. With suitable energy storage, utilities and grid management can couple producers and consumers with disparate temporal behaviors, thus reducing electric power peaks and the need of additional power generation plants. Energy storage could be implemented at grid level, or at user level.

In economic terms, a storage system with a discharge duration of a few hours results in a huge potential: storage is charged with low-value electric energy generated using renewable energy.

According to the research services of European Parliament [6], the energy storage is one of the top ten technologies that will drastically change our lives. There are several dominant types of energy storage currently in active development, typically grouped into four categories: electrical, mechanical, thermal and chemical. The chemical storage systems are wide spread and very effective for their relatively high energy density and flexibility. However, their environmental footprint is quite high, since they rely on precious and rare materials, they feature a pretty long charging time, and their life time is limited below ten years.

TABLE I
Main parameters for MechSTOR flywheel battery and for benchmark Lithium-Ion battery available in the Ecoinvent library.

Technology	Flywheel	Lithium-Ion battery
Materials	Steel	Li-Ion and metals
Weight (kg)	425	$30 \div 100$
Electrical Peak Power (kW)	5	5
Storage capacity (kWh)	3	3
Energy density (Wh/kg)	$\simeq 7$	$\simeq 50 \div 150$
Photovoltaic system (kW)	3	3
Expected life (years)	30	10

On the other side, mechanical storage systems feature a quite immediate charging time and are characterized by a smaller environmental footprint. Compared to chemical systems, the advantages of mechanical storage are: a simpler production process; opportunity to re-use or recycle materials; immediate charging time; and longer life time. However, the energy density of mechanical systems is lower and the discharge duration is a critical issue. Flywheel batteries are mainly designed for peak shaving in energy distribution systems. The flywheel storage capacity depends on the moment of inertia and squared angular speed. In order to reach a typical household energy capacity, an high rotational speed and high discharge duration are required.

Here, a flywheel for distributed energy storage was designed for a household application with a photovoltaic system.

III. Electric Motor/generator specifications

The electrical machine and its mechanical structure such as bearings, joint, vacuum system, are the key design devices in a flywheel storage system. Mechanical and electrical machine losses must be minimized, in order to achieve a self-discharge duration of a few hours. Existing flywheel based energy storage system are usually designed for peak shaving in grid quality system, and they feature high size and very low discharge duration: about a few seconds with stored energy around 10 MW.

Some commercial flywheel applications adopt a synchronous reluctance machines in order to avoid self-braking even when machine supply is disconnected, other solutions, for the same reason, rely on induction machines [7], [8].

This paper presents an application for a distributed energy storage system of few kW at household level and with a self-discharge duration of a few hours, in order to achieve the renewable energies time-shift specifications. The design must take into account also the total cost of the system that

This article has been accepted for publication in a future issue of this journal, but has not been fully edited. Content may change prior to final publication. Citation information: DOI 10.1109/TIE.2020.3026292, IEEE Transactions on Industrial Electronics

should be compliant with the requirements of an household application.

Table I reports performances of MechSTOR versus reference Li-Ion batteries, being the latter much better in terms of energy density. However, flywheel storage features a much longer lifetime and does not require precious raw materials. Moreover, the flywheel battery parts can be easily replaced and recycled resulting in a much circular process. On the other hand, the chemical battery requires complex manufacturing and recycling process. In summary, ownership cost and emissions are lower for the flywheel battery.

The flywheel is based on a steel cylinder structure and the storage capacity was chosen for a single user connected to the grid with a photovoltaic system on the roof.

The nominal rotational speed of the flywheel, and consequently of the electrical machine, has been chosen by using typical floor area and volume of an household appliance, and by the constraints on centrifugal stress. Specifically, its volume is less than 1.5 m^3 and its floor area is less than 1 m^2. A rated rotational speed of 9000 rpm ($\omega_m = 942\ rad/s$) was chosen, and its parameter are computed according to the theoretical kinetic energy relationship (1).

Machines at higher speed were investigated, up to 36.000 rpm for synchronous reluctance machines, [9]. However, the rated speed was set at 9000 rpm for two main reasons: (1) at higher speed, special materials, deep vacuum and magnetic bearings are required; (2) results in [9] show that at higher speed saliency ratio and power factor are largely decreased. The design analysis here reported is aimed at low-cost machines for flywheel battery, where energy optimisation and material choices are key issues.

$$U = \frac{1}{2} J \omega_m^2 \tag{1}$$

where $J = \pi \rho R^4 h/2$ is the mass moment of inertia of the cylinder disc, ρ is the density of the material and ω_m is the rotational speed in rad/s.

At 9000 rpm, with a wheel radius of $R = 0.34\ m$, wheel height of $h = 0.15\ m$ and a material density of $\rho = 7850\ kg/m^3$ the theoretical kinetic energy is:

$$U \simeq 10 \text{ MJ} \simeq 3.1 \text{ kWh} \tag{2}$$

IV. Machines Design and Comparison

A. Energy efficiency and self-discharge duration

The optimal design of an electrical machine for flywheel batteries must fulfill two different benchmarks: (1) energy efficiency η_1, that is the classical definition of energy conversion from electric to mechanic energy and vice versa and (2) self-discharge duration t_{sd} that depends on the rotational losses at no load and thus on the capability of retaining energy when the grid is disconnected from the flywheel battery.

The two benchmarks are contradictory, since they require different design choices. The efficiency η_1 would lead to a machine design that maximizes the machine self-capability to produce magnetic flux (i.e. permanent magnet), in order to avoid magnetizing current in the stator windings and related

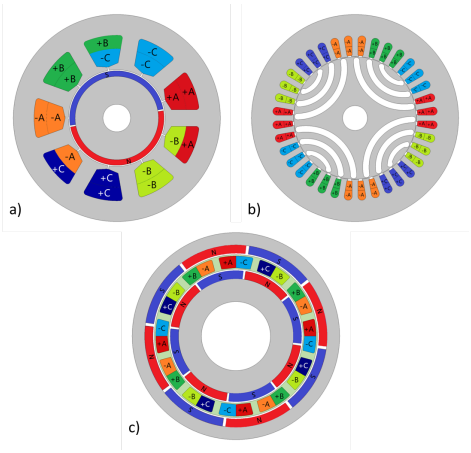

Fig. 1. Geometry comparison of the studied configurations and their winding scheme.

Joule losses. Hence, high values of η_1 could be achieved by permanent-magnets and magnetic circuits with low reluctance. The main drawbacks of iron-core machine are the core losses caused by hysteresis and eddy currents. At no load, losses caused by permanent magnets and eddy currents could heavily affect the self-discharge duration because of their self-braking effect even when the power supply is disconnected. For flywheel batteries, self-discharge duration is one the most important requirement, that will be used as the main reference for design choices. In the following, iron-core losses will be considered a benchmark for self-discharge duration.

Hereafter, the performances of three different machines are compared by Finite Element Analysis (FEA). Specifically, the proposed ironless dual-rotor SPM is compared with two traditional iron-core synchronous machines: a surface permanent-magnet (SPM) machine and a pure reluctance machine.

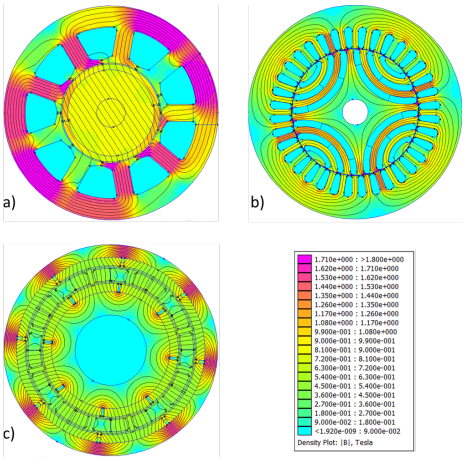

Fig. 2. Magnetic flux density distribution of: a) SPM_{IC}, b) SyncRel and c) SPM_{IL}.

The comparison is made fixing some constraints, and is based on the two benchmarks η_1 and t_{sd} above defined. The common constraints are the external diameter of the machine and the torque. An external diameter of 150 mm and 3 Nm torque were fixed, in order to design a motor/generator

This article has been accepted for publication in a future issue of this journal, but has not been fully edited. Content may change prior to final publication. Citation information: DOI 10.1109/TIE.2020.3026292, IEEE Transactions on Industrial Electronics

consistent with the parameters of Table I.

Figure 1 shows two-dimensional (2D) geometries and winding arrangements of the iron-core SPM machine (referred to as SPM_{IC}), the synchronous reluctance (SyncRel) machine and the ironless dual-rotor machine (SPM_{IL}).

The main goal of SPM_{IC} design was the reduction of iron-core losses, thus improving its performance during self-discharge operation. Hence, a special non-oriented electric steel NO20 has been chosen because of its low core density losses. The slot-pole combination is another critical parameter that affects machine performances, [10], [11], [12], [13].

A 9-2 slot-pole combination was chosen, the corresponding winding arrangement is derived from the star of slot theory and it is show in 1a). The 9-2 combination allows minimizing the electric frequency f_{el}, by reducing the number of pole pairs (3). A single pole pair corresponds to a minimum of iron-core losses, that are directly proportional to electric frequency, according to Steinmetz's equations: (4). Moreover, it corresponds to a minimum of eddy current losses (5).

$$f_e = p \cdot f_m \tag{3}$$

$$P_{Fe_{hyst}} = k_{hist} \cdot f_e \cdot B_M^k \tag{4}$$

$$P_{Fe_{ec}} = k_{ec} \cdot f_e^2 \cdot B_M^k \tag{5}$$

The SyncRel machine was designed with a 36-4 slot-pole combination, with silicon-iron electric steel M330-35A for stator and rotor laminations.

Figure 2 shows the flux density distribution at rated load of SPM_{IC} (a) and $SyncRel$ (b) assuming the same colour scale for flux density range. The magnetic flux density of SPM_{IC} is the highest because of PMs.

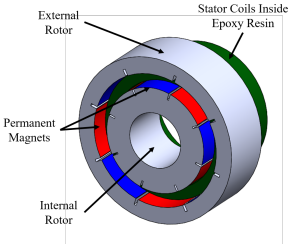

Fig. 3. CAD sketch of MechSTOR rotor.

For the SPM_{IL} machine, a ironless dual-rotor SPM synchronous machine topology is here proposed. The lack of iron reduces self-discharge of the machine when the grid is disconnected from flywheel battery, i.e. when the machine is spinning without connection to supply or load. Moreover, the design was optimized by FEA in order to achieve power and torque density as high as those of a iron-core machine with the same constraints, as detailed in the next subsection.

The dual-rotor configuration of SPM_{IL} minimizes Magneto-motive force (MMF) drops by reducing the reluctance of magnetic paths. It is made of two concentric circular structures with surface mounted permanent magnets, while

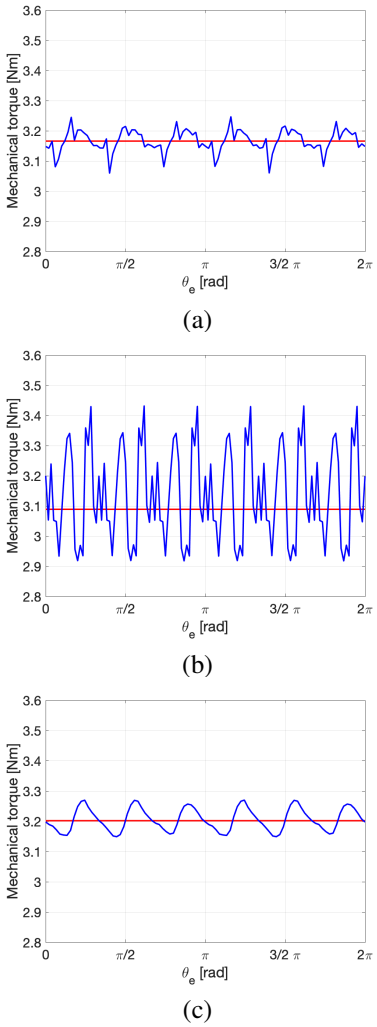

Fig. 4. Mechanical (blue line) and median (red line) Torque of SPM_{IC} (a), SyncRel (b) and SPM_{IL} (c) as a function of electrical angle.

stator coils are placed between the rotors, as sketched in Figure 3.

For the SPM_{IL} machine, the 12-8 slot-pole combination was chosen because it is an optimal trade-off among: harmonic content of electromagnetic force (EMF); winding factor k_{fill}; and the electric frequency in the operating range. The dimensions of the stator slots and magnets were optimized in order to achieve the fixed constraints of torque and external diameter, as detailed in the next subsection; and to satisfy thermal constraints by a suitable choice of material copper losses per unit of stack.

Table II summarizes the geometrical parameters of the three reference machines, that have the same outer diameter of 150 mm. The $SyncRel$ has the longest lamination stack, while the SPM_{IC} the shortest one. Given the shortest lamination and the single pole pair, the SPM_{IC} has a lower PMs volume than SPM_{IL}.

The three machines are designed for a continuous power of 3 kW that corresponds at a continuous torque of about 3 Nm. Figure 4 shows the mean torque of the three machines that is close to the value fixed by constraints of about (3 Nm) as

This article has been accepted for publication in a future issue of this journal, but has not been fully edited. Content may change prior to final publication. Citation information: DOI 10.1109/TIE.2020.3026292, IEEE Transactions on Industrial Electronics

TABLE II
GEOMETRICAL PARAMETERS

SPM_{IC}		**SyncRel**	SPM_{IL}	
Stator External Diameter	150 mm	150 mm	Outer Rotor External Diameter	150 mm
			Outer Rotor Inner Diameter	132 mm
Stator Inner Diameter	90 mm	104 mm	Inner Rotor External Diameter	82 mm
			Inner Rotor Inner Diameter	55 mm
Lamination Stack	30 mm	53 mm	Lamination Stack	50 mm
Stator Slots	9	36	Stator Slots	12
Poles	2	4	Poles	8
PM Volume	$2.31 \cdot 10^{-5}$ m^3	0 m^3	PM Volume	$2.13 \cdot 10^{-4}$ m^3

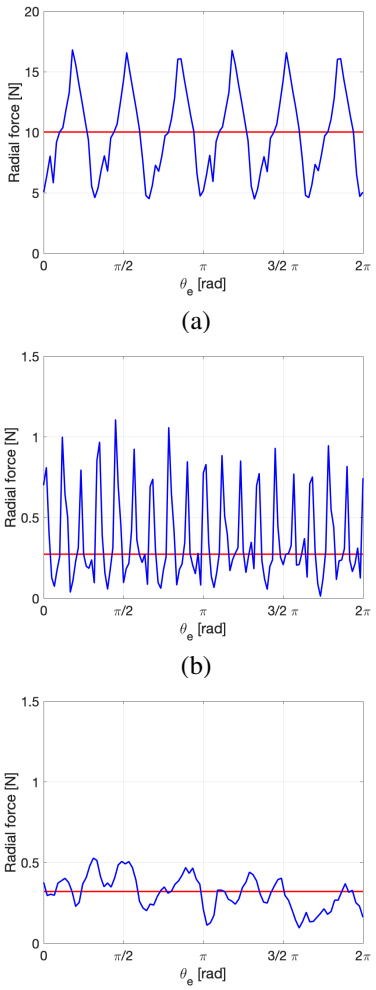

Fig. 5. Radial forces acting on the rotor of SPM_{IC} (a), $SyncRel$ (b) and SPM_{IL} (c) as a function of electrical angle. Different scales are used for the vertical axes.

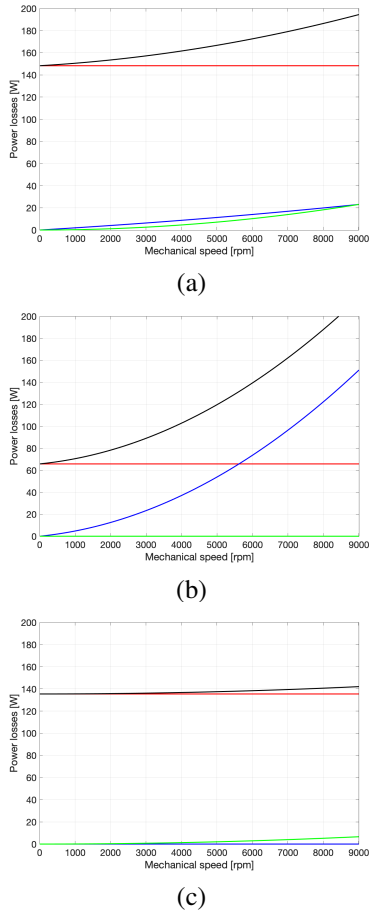

Fig. 6. Power losses of SPM_{IC} (a), SyncRel (b) and SPM_{IL} (c), as a function of mechanical speed at nominal current. Copper losses (red line), iron losses (blue line), permanent-magnet losses (green line) and total losses (black line).

a function of electrical angle θ_e. Different pole pairs P were used for the three machines: $P = 1$ for SPM_{IC}; $P = 2$ for $SyncRel$; $P = 4$ for SPM_{IL}.

As expected, the $SyncRel$ exhibits the highest torque ripple than the other ones.

Self-discharge duration t_{sd} is assessed by FEA of power losses and of radial forces at no load. Radial forces are an important parameter, as mechanical losses can be reduced by high performance bearings or magnetical bearings, that are strongly affected by radial forces. Radial forces are caused by unbalanced magnetic flux of the three machines.

Figure 5 show the radial forces at rated load for the three machines. Peak and mean values of radial forces are very diverse: from about 0.31 N for SPM_{IL} to about 9.978 N for SPM_{IC}. Hence, the wear of bearings is very different in the three machines. In case of small eccentricity of the rotor the ironless machine is less prone to radial unbalanced force increasing due to the intrinsic nature of the machine itself, while for the other two machine a small eccentricity of the rotor could produce a strong increase of the radial forces.

Power losses are caused by three main components: copper

This article has been accepted for publication in a future issue of this journal, but has not been fully edited. Content may change prior to final publication. Citation information: DOI 10.1109/TIE.2020.3026292, IEEE Transactions on Industrial Electronics

TABLE III
RESULTS OF FINITE ELEMENT ANALYSIS

	Efficiency [%] @ 9000 rpm 3kW η_1	**No Load Total Losses [W]**	**No Load Iron-Core Losses [W]**	**Power Factor Rated Load**	**Radial Force [N]**	**Net Annual Energy [kWh]**
SPM_{IC}	93.7	25	20	0.87	9.98	4318
$SyncRel$	93.2	Almost zero	Almost zero	0.69	0.37	4473
SPM_{IL}	95.3	0.75	Almost zero	0.99	0.32	4574

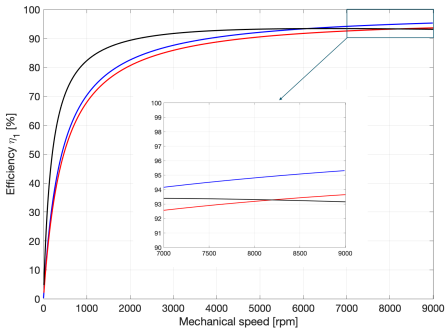

Fig. 7. Simulation results. Conversion efficiency η_1 of SPM_{IC} (red line), SyncRel (black line) and SPM_{IL} (blue line) as a function of mechanical speed at nominal current.

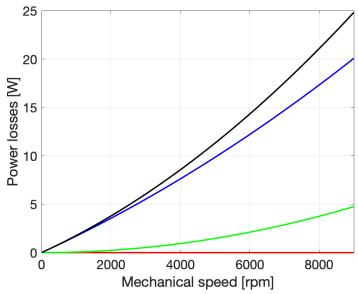

Fig. 8. Power losses at no load of SPM_{IC} machine as a function of mechanical speed. Copper losses (red line), iron losses (blue line), permanent-magnet losses (green line) and total losses (black line).

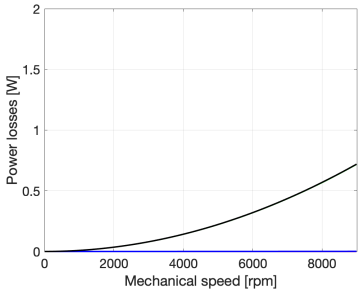

Fig. 9. Power losses at no load of SPM_{IL} machine as a function of mechanical speed. Copper losses (red line), iron losses (blue line), permanent-magnet losses (green line) and total losses (black line).

losses, iron-core losses, permanent magnet losses. The single components and the total losses are computed as a function of rotor mechanical speed. The power losses increase with the mechanical speed, with different behaviours, according to machine structure and features.

Fig. 7 compares the conversion efficiency η_1 for the three machines as a function of mechanical speed at nominal current (corresponding to nominal torque of $3Nm$). At rated speed of $9000\ rpm$ the conversion efficiency is of about $93.7\ \%$ for SPM_{IC}; $93.2\ \%$ for $SyncRel$; and $95.3\ \%$ for SPM_{IL}.

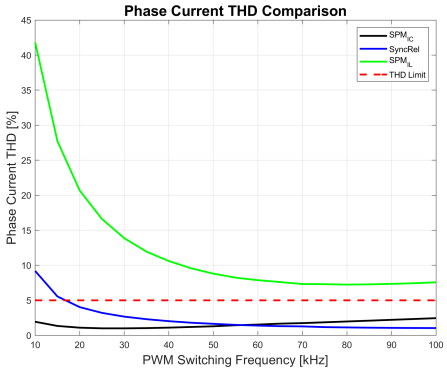

Fig. 10. Simulation results. Total harmonic distortion of machine current THD_i versus switching frequency. SPM_{IC} (black line), $SyncRel$ (blue line) and SPM_{IL} (green line). THD limit is reported in red dashed line

Fig. 11. Dual-rotor ironless surface permanent-magnet machine for MechSTOR prototype (left). Parts of the MechSTOR prototype starting from left side: stator, inner rotor, external rotor (right).

Iron-core losses were computed at no load for the three machines. For $SyncRel$ machine iron-core losses are negligible, because of the absence of permanent magnets. On the other hand, in SPM machines iron-core losses are mainly caused by PMs. Figures 8 and 9 show the iron-core losses of SPM_{IC} and SPM_{IL} at no load, respectively. Fig. 9 shows that only permanent magnet losses are non negligible for SPM_{IL} at no load. Iron-core losses of SPM_{IL} at $9000\ rpm$ and at no load are remarkably lower than those of SPM_{IC}, table III. For a typical household with a flywheel battery of 5 kW the performances are summarized in table III. The flywheel battery will operate continuously, hence, the difference in terms of power losses between iron-core and ironless machine will result in an annual energy savings, as detailed in section V.

This article has been accepted for publication in a future issue of this journal, but has not been fully edited. Content may change prior to final publication. Citation information: DOI 10.1109/TIE.2020.3026292, IEEE Transactions on Industrial Electronics

B. Dual-rotor ironless machine design optimization

The design of the ironless SPM machine was optimized by Finite Element Analysis (FEA) in order to: achieve performances close to iron-core machines; minimize electrical machine losses; and meet the specifications of Table I. The dual-rotor ironless SPM configuration increases the magneto motive force (MMF) provided by the permanent-magnet and reduces the flux path reluctance providing a second yoke on the internal side of the machine. The authors of papers [14], [15], [16] propose other different configurations of ironless permanent-magnet machines for flywheel applications.

The key parameter in a dual-rotor ironless machine is the gap between the internal and external rotor. The increase of gap length leaves more room for stator coils, however, it also enhances the magnetomotive force drop in the air gap. A nice trade-off between this specifications is the main purpose of the optimization design procedure, aiming at selecting the geometry of machine, with special reference to the length of the gap between the internal and external rotor.

A series of simulations were carried out keeping constant the external diameter to $150\ mm$ and modifying the stator coils height. Two types of tests were made: in the former, the current density in the slots was kept constant; while in the latter, the total Joule losses were kept at a constant value. The results were reported in Fig. 12 and 13 that report the mean torque versus the stator slot height. With constant current density, simulations show that the maximum value of torque saturates at about $4.8Nm$ with a stator slot height higher than 10 mm.

With constant Joule losses, the torque will decrease increasing the stator slot height. A trade-off of 8.5 mm was chosen, based on the minimum stator slot height value that leaves rooms for manufacturing with suitable current density.

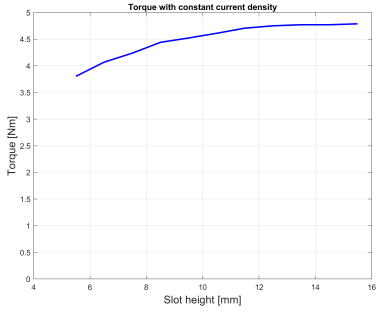

Fig. 12. Torque profile versus slot height with constant current density.

C. Drives performances

The motor/generator of a flywheel battery shall be operated by a power converter. The three machines were regulated by a vector control in dq axis obtained by Park transformation.

Performances of machines operated by a power converter are fairly assessed by the total harmonic distortion of the output current (THD_i). This parameter is proportional to copper losses, iron losses and overcurrents. Moreover, a low THD of currents limits electromagnetic emissions. The machines

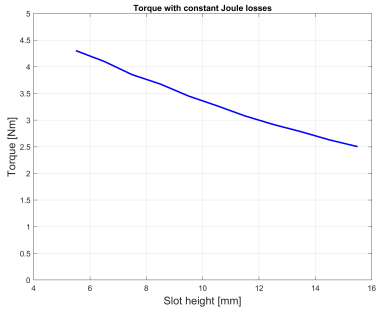

Fig. 13. Torque profile versus slot height with constant Joule losses.

TABLE IV
RESISTANCE AND INDUCTANCES

	Phase Resistance [Ω]	Synchronous Inductances [mH]
SPM_{IC}	2.6	1
$SyncRel$	0.386	L_{sd} = 3.53 L_{sq} = 32
SPM_{IL}	0.914	20

were operated at fixed mechanical torque (3 Nm) and at fixed mechanical speed (9000 rpm), with a DC bus voltage of 700 V. Machine resistance and inductance were designed in order to achieve these constraints, their optimal values were chosen by FEA and are reported in table IV. Machine comparison is made by the analysis of total harmonic distortion of phase currents (THD$_i$) as a function of switching frequency of the power converter f_{sw}. The comparison is made fixing to maximum value of THD$_i$ at 5 %. Each machine achieves this constraint at a different value of switching frequency. THD$_i$ is computed by PLECS simulations, that was used to model machine, power converter and vector control scheme.

The machines resistance and synchronous inductance were computed by FEA and were set as motor parameter the PLECS simulation in order to obtain the same rated performance of FEA. Table IV sums up the machines parameters values. PLECS simulations were carried out over a range of switching frequencies from $10\ kHz$ to $55\ kHz$ with a step of $5\ kHz$ at rated condition. Figure 10 shows the total harmonic distortion of machine output current versus the switching frequency of the power converter.

Simulation results show that the proposed SPM_{IL} machine shall be operated at a switching frequency as high as $65\ kHz$, in order to reduce the THD$_i$ at minimum level. In summary, the SPM_{IL} machine can be used for flywheel batteries only with suitable input filters and with a switching frequency higher than $65KHz$. Hence, multi-level power converters are recommended for the power converter used with the MechSTOR prototype.

V. ENERGY STORAGE POTENTIAL: A BENCHMARK FOR MACHINE SELECTION

The three machines feature diverse and often contrasting performances. Hence, a benchmark is here defined to select the optimal machine, based on annual energy storage capability.

This article has been accepted for publication in a future issue of this journal, but has not been fully edited. Content may change prior to final publication. Citation information: DOI 10.1109/TIE.2020.3026292, IEEE Transactions on Industrial Electronics

The three machines can be compared in terms of annual energy given the same source. Let us assume that the three reference machine are supplied with a identical flywheel with 3 kW of mechanical energy, and that a power converter with identical size is used for the connection to the common DC bus, fig. 14. The annual net energy stored by the flywheel battery E_{TOT} depends on the machine parameters: efficiency during motor or generator operation, and no load losses. Neglecting mechanical losses, the annual net energy can be computed as follows, assuming that the machine operates only at rated conditions.

$$E_{TOT} = P_m \cdot \eta_1 \cdot h_1 - P_{NLlosses} \cdot h_i \tag{6}$$

where P_m is the rated machine power equal to 3 kW, η_1 is the efficiency of the machine, $P_{NLlosses}$ are the no load losses of the machine in W, $h_1 = 1600$ is the number of hours of operation with load and $h_i = 7160$ is the numbers of hours of operation time at no load.

Results are reported in the column *Annual energy* of table III. The power factor of the machines has a further impact on inverter size and cost, and on efficiency, even if it is not taken into account in this comparison.

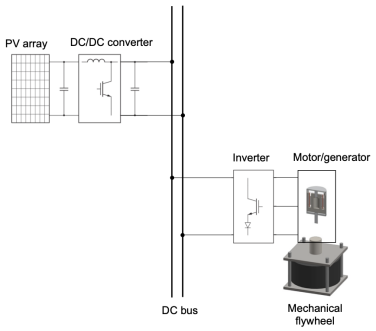

Fig. 14. Block diagram of the power system for a household. Electrical loads and other converters are connected to the common DC bus.

Hence, the energy stored with the ironless machine is higher than the other reference machines.

In summary, FEA results show that the proposed SPM_{IL} machine outperforms the others machines in terms of efficiency, power factor and radial unbalanced forces, therefore is the best suited for a household flywheel storage energy system. SPM_{IL} has the best performances in terms of energy conversion η_1 and very low power losses during self-discharge condition. It features higher total harmonic distortion of current. The SPM_{IC} has the highest power density, but due to its iron-core structure has low performance in terms of η_1 and self-discharge duration at rated condition. The $SyncRel$ features the highest performances in terms of self-discharge duration, however, its conversion efficiency at rated speed is the lowest. In terms of annual net energy, the difference between the ironless machines and iron-core machines is of about 200 kWh, that is more than 5% of the average electrical energy consumption of an household, table III.

Hence, the ironless dual-rotor configuration was chosen for the MechSTOR prototype.

VI. Experimental results

The prototype of the dual-rotor ironless permanent-magnet machine was realized and tested in order to validate FEA simulation results of SPM_{IL} machine, Figure 11. Figure 11-right shows stator, inner and outer rotor pictures.

The stator was manufactured with magnetic wire rounded on a jig in order to achieve the desired winding configuration and filling factor, then stator winding were encapsulated with epoxy resin and reinforced with a special nylon fiber, in order to achieve a superior structural strength and to handle the form variations occurring during the cooling-down process. The end windings of each coil were connected outside the rear flange, fig. 15, thus allowing different series or parallel connections (from zero to four parallel connections). Hence, the performances of the machine at low speed can be experimentally investigated by changing the number of equivalent series turns without rewinding the stator coils. The permanent-magnet are in Neodymium Iron Boron, $NdFeB$.

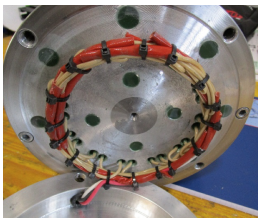

Fig. 15. MechSTOR motor/generator coil connections.

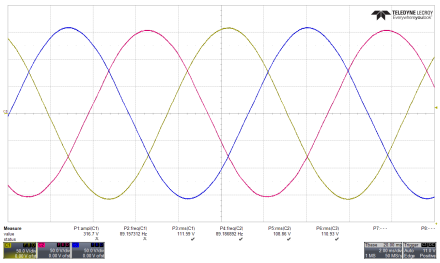

Fig. 16. Waveforms of electromotive force of the MechSTOR prototype.

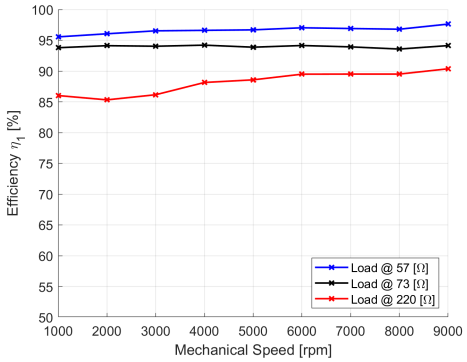

Fig. 17. Experimental results. Efficiency of MechSTOR prototype used as a generator with different pure three phase resistive loads, including mechanical losses compensation. Resistive load at 25.6 Ω (red line), 57 Ω (blue line), 73 Ω (black line).

TABLE V
EFFICIENCY COMPARISON AT RATED SPEED FEA AND EXPERIMENTAL

	Efficiency @ 9000 r/min	**Torque [Nm]**
FEA	95.30	$3Nm$
Experimental results at 57 Ω	97.63	$9.52Nm$
Experimental results at 73 Ω	94.14	$7.96Nm$
Experimental results at 220 Ω	77.8	$5.63Nm$

The prototype of dual-rotor ironless SPM machine was tested in order to validate the proposed SPM_{IL} machine. The prototype was operated only as a generator. Motoring would require a complex setup for power electronics and mechanical flywheel. The ironless machine was mechanically connected to a prime mover, an induction machine controlled by a speed control loop, that mimics the mechanical flywheel providing the input mechanical power. The mechanical parameters were measured with a torque meter placed at the mechanical coupling of the two machines. Three different resistive three-phase loads were connected to the MechSTOR prototype: $26.5\ \Omega$, $57\ \Omega$ and $73\ \Omega$. The tests were performed over a speed range from $1000\ rpm$ to the nominal speed of $9000\ rpm$, with a $1000\ rpm$ step. At $26.5\ \Omega$ load the maximum speed was limited to $5000\ rpm$ by over current limitations. For each sample, voltages, current and power components were measured by a three-phase power analyzer.

Figure 16 shows the waveforms of three-phase electromotive forces measured from the MechSTOR prototype operated as a generator. Experiments show that the efficiency η_1 of the MechSTOR prototype is quite constant for each resistor value, over a wide mechanical speed range, a very important feature for the flywheel battery that is operated in a wide mechanical speed range. On the other hand, at nominal speed, experimental efficiency is lower that simulated efficiency, i.e. $86\ \%$ instead of $96\ \%$.

This difference is caused by the low quality mechanical bearings used for the prototype. A no load test was made, that shows that losses are proportional to the square of mechanical speed, with a dominant mechanical component. This additional mechanical losses were removed from the experimental results, assuming that the final prototype will use high-performance low-friction mechanical bearings or magnetic bearings. Experimental results, removing the mechanical bearings bias, are reported in fig. 17.

Table V compares simulation and experimental results of efficiency at rated speed. The difference is caused by some phenomena that are not modeled by FEA simulations: friction and mechanical shaft losses. Moreover, the difference between experiments and FEA is caused by the different impedance matching between the different loads and the motor-generator. On the other hand, FEA are based on active current control, where the current are fixed in phase with the back emf.

VII. CONCLUSIONS

This paper investigates the design of a motor/generator for flywheel batteries, used for distributed energy storage at household level. Three different machine configurations were designed and compared, and a prototype of the machine with best performances was optimized and realized.

The comparison was made fixing some common performances: torque and size, and is based on the specification of a typical household power system with a photovoltaic. FEA was used to compare the three reference machine: a SPM iron-core machine, a SPM ironless dual rotor machine and a synchronous reluctance machine. The ironless machine is best suited for the flywheel battery. It features higher efficiency at high speed, lower losses, and much lower radial forces, that heavily affect the bearing system. High radial forces result in higher self-discharge duration, a key parameter for renewable energy time-shift value proposition.

A prototype of the ironless machine (MechSTOR) was realized and tested. Results show that the MechSTOR prototype achieves a conversion efficiency of about $95\ \%$ in a wide mechanical speed range from $1000\ rpm$ to the nominal speed of $9000rpm$ for different loads.

On the other hand, iron-core machines would require a shorter lamination stack and lower permanent-magnet volume, also because of the lower number of magnetic poles. However, the core losses of iron-core SPM machine at no load and nominal speed are about $25\ W$, reducing the energy storage potential. The synchronous reluctance machine features higher power density and does not require permanent magnets. However, its performances are much less than ironless machine, in terms of efficiency and power factor.

REFERENCES

[1] Deloitte, "Energy storage: Tracking the technologies that will transform the power sector," 2015. [Online]. Available: https://www2.deloitte.com/us/en/pages/consulting/articles/energy-storage-tracking-technologies-transform-power-sector.html[accessed28.4.18]

[2] J. E. G. Corey, "Energy storage for the electricity grid: Benefits and market potential assessment guide. a study for the DOE energy storage systems program," *Sandia Report*, 2010.

[3] R. Hebner, J. Beno, and A. Walls, "Flywheel batteries come around again," *IEEE Spectrum*, vol. 39, no. 4, pp. 46–51, April 2002.

[4] C. Bianchini, A. Bellini, D. David, and A. Torreggiani, "Ironless dual-rotor permanent magnet machine for flywheel batteries," in *Proceedings of IEEE Energy Conversion Congress & Expo, ECCE 2018*, september 2018.

[5] O. e. a. Edenhofer, "Summary for policymakers. in: Climate change 2014: Mitigation of climate change. contribution of working group III to the fifth assessment report of the intergovernmental panel on climate change," *IPCC*, no. 4, 2014.

[6] L. V. Woensel and G. Archer, "Ten technologies that could change our lives. potential impacts and policy implications," *European Parliamentary Research Service*, January 2015.

[7] H. Akagi and H. Sato, "Control and performance of a doubly-fed induction machine intended for a flywheel energy storage system," *IEEE Transactions on Power Electronics*, vol. 17, no. 1, pp. 109–116, January 2002.

[8] G. Cimuca, S. Breban, M. M. Radulescu, C. Saudemont, and B. Robyns, "Design and control strategies of an induction-machine-based flywheel energy storage system associated to a variable-speed wind generator," *IEEE Transactions on Energy Conversion*, vol. 25, no. 2, pp. 526–534, June 2010.

[9] C. Babetto, G. Bacco, and N. Bianchi, "Synchronous reluctance machine optimization for high-speed applications," *IEEE Transactions on Energy Conversion*, vol. 33, no. 3, pp. 1266–1273, 2018.

[10] N. Bianchi and S. Bolognani, "Design techniques for reducing the cogging torque in surface-mounted pm motors," *IEEE Transactions on Industry Applications*, vol. 38, no. 5, pp. 1259–1265, Sep. 2002.

[11] I. Abdennadher, A. Masmoudi, M. Castiello, and N. Bianchi, "On the effect of the rotor polarity on the performance of fractional slot spm machines," in *2015 International Conference on Sustainable Mobility Applications, Renewables and Technology (SMART)*, Nov 2015, pp. 1–6.

[12] B. Boazzo, G. Pellegrino, and A. Vagati, "Multipolar spm machines for direct-drive application: A general design approach," *IEEE Transactions on Industry Applications*, vol. 50, no. 1, pp. 327–337, Jan 2014.

[13] A. Torreggiani, C. Bianchini, M. Davoli, and A. Bellini, "Design for reliability: The case of fractional-slot surface permanent-magnet machines," *Energies*, vol. 12, no. 1691, May 2019.

[14] K. Liu, X. Fu, M. Lin, and L. Tai, "AC copper losses analysis of the ironless brushless dc motor used in a flywheel energy storage system," *IEEE Transactions on Applied Superconductivity*, vol. 26, no. 7, pp. 1–5, October 2016.

[15] I. M. Higginson, H. Hess, and J. D. Law, "Ironless permanent magnet synchronous machine stiffness calculations for flywheel energy storage systems," *2011 IEEE International Electric Machines and Drives Conference (IEMDC)*, pp. 1357–1362, 2011.

[16] S. M. Jang, D. J. You, K. J. Ko, and S. K. Choi, "Design and experimental evaluation of synchronous machine without iron loss using double-sided halbach magnetized pm rotor in high power FESS," *IEEE Transactions on Magnetics*, vol. 44, no. 11, pp. 4337–4340, November 2008.

Claudio Bianchini , PhD, was born in Italy on September 9, 1974. He received the Master degree in Management Engineering at the University of Modena and Reggio Emilia in 2002, the Bachelor degree in Mechatronic Engineering in the 2006 and the Ph.D. in 2010 from the same University. He was an honorary scholar at the University of Wisconsin, Madison, during 2008. He is an Assistant Professor at Department of Engineering "Enzo Ferrari", University of Modena and Reggio Emilia, Italy. His research interests include electrical machines design, control and diagnostic, linear electrical machines, permanent magnet machines. He is also a member of the Italian standard committee for electric machines and he is the director of the Electric Motor Laboratory at Reggio Emilia Innovazione since 2012. He is author or co-author of more than 40 international papers, he holds two WPO patent in the fields of electrical machines and mechatronic application.

Ambra Torreggiani was born in Italy in 1990. She received Bachelor and Master degrees in Management Engineering from the University of Modena and Reggio Emilia, Italy, in 2012 and 2015 respectively. She received PhD in Industrial Innovation Engineering from the University of Modena and Reggio Emilia, Italy in 2019. From June 2019 to September 2019 she was a PhD visiting student by the University of Nottingham, UK where she worked on a research topic related to iron steel characterization for high speed electrical machines in automotive application. Since 2019 she works in Raw Power Srl, Reggio Emilia, Italy, in research and development on the design of electrical machines. She collaborates with the DIEF department of the University of Modena and Reggio Emilia, Italy. Her research topics are on the electrical synchronous machine design and electric machines control.

Danilo David was born in Italy in 1979. He received Master degree in Electronic Engineering from the University of Parma, Italy in 2007. His main research topics are power electronics, electric machines control industrial automation and power delivery system. Since 2016, he collaborates with Raw Power Srl, Reggio, Italy in research and development of electrical machine control systems.

Alberto Bellini (S'96-M'99-SM'18) was born in Italy in 1969. He received the Laurea (M.S.) degree in electronic engineering and the Ph.D. degree in computer science and electronics engineering from the University of Bologna, Bologna, Italy, in 1994 and 1998, respectively. From 1999 to 2004, he was with the University of Parma, Parma, Italy. He was an Honorary Scholar with the University of Wisconsin, Madison, WI, USA, in 2000. From 2004 to 2013, he was with the University of Modena and Reggio Emilia, Reggio Emilia, Italy. Since 2013, he has been a Professor of electric machines and drives with the Department of Electrical Engineering, University of Bologna. He is the author or coauthor of more than 100 papers and one textbook and is the holder of three industrial patents. His research interests include electric drive design and diagnosis, power electronics, and signal processing for industrial applications and sustainability. He was the recipient of the First Prize Paper Award from the Electric Machines Committee of the IEEE Industry Applications Society in 2001.